Analytical Performance of a Molecularly Imprinted Polymer-Based Potentiometric Sensor for the Antibiotic Meropenem

Herlina Herlina[1*], Ahmad Hafizullah Ritonga[1], Andy Febriady[1], Asvia Rahayu[1], Barita Aritonang[1], Muhammad Razali[2], Reynaldo Sinaga[1], and Amelia Sundari[1]

[1]*Institut Kesehatan Medistra Lubuk Pakam, Jl. Sudirman No. 38, Petapahan, Lubuk Pakam, Deli Serdang 20512, Indonesia*

[2]*Universitas Pembinaan Masyarakat Indonesia, Jl. Balai Desa, Pasar 12, Marindal Dua, Patumbak, Deli Serdang 20149, Indonesia*

* ***Corresponding author:***

email: herlina@medistra.ac.id

Received: January 22, 2026
Accepted: April 4, 2026

DOI: 10.22146/ijc.115916

Abstract: *Accurate determination of meropenem is essential for therapeutic drug monitoring and pharmaceutical quality control. In this study, a molecularly imprinted polymer (MIP)-based potentiometric ion-selective electrode was developed for selective detection of meropenem. The MIP was synthesized via bulk free-radical polymerization and characterized using FTIR, SEM, and TGA, confirming the formation of a stable polymer matrix. The polymer was incorporated into a PVC membrane to fabricate the sensor, and its analytical performance was evaluated. The sensor exhibited a near-Nernstian slope of 54.87 mV per decade and good linearity over the concentration range of 1.0×10^{-5}–1.0×10^{-3} M with a coefficient of determination (R^2) of 0.995. The calculated LOD and LOQ values were 1.12×10^{-5} and 1.43×10^{-5} M, respectively. The sensor showed a fast response time (~45 s) and optimal performance at pH 5.0–6.0. Selectivity evaluation using the matched potential method indicated moderate selectivity, with observable interference from structurally similar compounds. The sensor maintained stable performance for up to 50 days. These results demonstrate that the developed MIP-based potentiometric sensor provides a simple, cost-effective platform for meropenem detection and has potential for future applications following validation in real samples.*

Keywords: *molecularly imprinted polymer; potentiometric sensor; meropenem; ion-selective electrode; Nernstian*

■ INTRODUCTION

The increasing global consumption of antibiotics in human and veterinary medicine has led to their widespread presence in the environment, particularly in aquatic systems. This raises concerns regarding ecological impacts and the potential role of antibiotic residues, including meropenem, in promoting antimicrobial resistance [1]. Meropenem is a broad-spectrum carbapenem antibiotic commonly used to treat severe infections caused by multidrug-resistant bacteria. Due to its extensive clinical use, particularly in hospital settings, a fraction of administered doses may be excreted unmetabolized and enter wastewater systems. Consequently, the accurate determination of meropenem in pharmaceutical, environmental, and biological matrices is important for therapeutic monitoring and environmental risk assessment [2-3]

A range of analytical methods has been developed for the determination of meropenem. Chromatographic techniques, such as high-performance liquid chromatography (HPLC), are widely used due to their reliability and accuracy. For example, Ren et al. [4] reported an HPLC method for the simultaneous determination of meropenem and vaborbactam in plasma. More advanced techniques, including LC–MS/MS, provide higher sensitivity and selectivity and have been successfully applied to trace-level analysis in complex matrices such as serum and wastewater [4–6]. However, these methods generally require sophisticated instrumentation, extensive sample preparation, and

skilled operation, which may limit their use in routine or on-site applications

Liquid chromatography–tandem mass spectrometry (LC–MS/MS) offers the highest sensitivity and selectivity among chromatographic techniques. Jin et al. successfully developed a UPLC–MS/MS method with extremely low detection limits for meropenem in serum and cerebrospinal fluid, making it suitable for therapeutic drug monitoring (TDM) [7]. In addition, Wilk et al. [7] applied SPE–LC–MS/MS for the determination of meropenem in hospital wastewater, achieving high sensitivity at the ng/L level. Despite these advantages, LC–MS/MS is limited by very high equipment costs, the requirement for skilled operators, and limited suitability for rapid or routine testing.

Ultraviolet-visible (UV–vis) spectrophotometry has been employed as a straightforward and cost-effective method, particularly for pharmaceutical formulations. Narala and Saraswathi [8] reported a validated extractive spectrophotometric method for pharmaceutical formulations, while Mahmood and Mahmood [9] introduced a sensitivity-enhanced spectrophotometric approach through reagent optimization. However, UV-vis spectrophotometry suffers from limited selectivity and is generally unsuitable for complex biological matrices.

Electrochemical techniques have consistently demonstrated high sensitivity and reliability in the analysis of drugs in biological fluids and pharmaceutical formulations [10]. A novel GC/Gr/CNT-HQ/Fe-Ni electrochemical sensor for the simultaneous detection of the pneumonia drugs linezolid (LN) and meropenem (ME) in human serum. Leveraging the synergistic effects of its composite materials, the sensor achieved remarkably low detection limits (0.97 nM for LN and 1.3 nM for ME) and demonstrated excellent stability, high interference resistance, and the additional capability to concurrently detect theophylline (TH) [11]. Additional investigations using differential pulse voltammetry (DPV) with carbon nanotube-modified basal pyrolytic graphite electrodes showed a notable increase in the oxidation peak current of meropenem, with a linear range of 3.0×10^{-7} to 7.0×10^{-5} M and a detection limit of 1.5×10^{-6} M in human plasma samples. These results confirm that altering nanomaterials can significantly enhance the electrochemical sensing performance for meropenem [12].

Other electrochemical methods using carbon paste electrodes (CPEs) modified with bimetallic Cu/Ni metal-organic frameworks (MOFs) have also shown a significant increase in meropenem oxidation currents. The responses are linear over the range 5.0×10^{-7} to 1.16×10^{6} M in plasma samples, and the detection limit is about 1.16×10^{-6} M. These findings underscore the capacity of MOF-based materials to enhance voltammetric sensitivity to meropenem [13].

Potentiometric ion-selective electrodes (ISEs) represent an attractive alternative due to their simplicity, low cost, and rapid response. These sensors operate based on potential changes in ion activity and can be used for portable and on-site analysis. Nevertheless, conventional ISEs often suffer from limited selectivity, particularly when detecting structurally similar pharmaceutical compounds, which restricts their application in complex matrices [14-15].

Molecularly imprinted polymers (MIPs) have emerged as promising recognition elements that enhance selectivity in chemical sensing systems. MIPs are synthetic polymers prepared in the presence of a template molecule, resulting in specific binding sites complementary in size, shape, and functional groups to the target analyte. Compared to biological recognition elements, MIPs offer advantages such as chemical stability, reusability, and resistance to harsh environmental conditions [16].

The integration of MIPs into potentiometric sensors has been explored as a strategy to improve analyte recognition in ion-selective electrode systems. Although MIP-based potentiometric sensors have been reported for various pharmaceutical compounds, studies specifically focused on meropenem remain limited. Furthermore, comprehensive evaluation of analytical performance, particularly selectivity, response behavior, and operational stability, remains relatively scarce. Therefore, further investigation is required to assess the applicability of this approach for the detection of meropenem [17].

MIP technology is increasingly used to detect various analytes, but few studies focus on meropenem. Moreover, a comprehensive assessment of the analytical performance of MIP-based potentiometric sensors, including linearity, detection limits, pH influence, response time, operational lifespan, and stability, has yet to be documented. These limitations highlight the need for an alternative sensing strategy that provides selective, rapid, and reliable detection of meropenem.

Although various analytical methods have been reported for the determination of meropenem, most electrochemical approaches rely on voltammetric techniques using nanomaterial-modified electrodes, which often require complex fabrication and instrumentation. In contrast, the present study proposes an alternative approach by integrating MIPs with a potentiometric ion-selective electrode system, thereby providing a simpler sensing platform. The novelty of this work lies not only in the application of MIP-based potentiometric sensing for meropenem detection, which remains limited, but also in the systematic evaluation of its analytical performance, including selectivity assessment using the matched potential method (MPM), response behavior, and operational stability. This approach provides an alternative analytical strategy that emphasizes simplicity and practical applicability while maintaining acceptable analytical performance compared to more complex electrochemical methods.

■ EXPERIMENTAL SECTION

Materials

Meropenem trihydrate (analytical grade) was used as the template molecule, purchased from Bernofarm Laboratories. Methyl methacrylate (MMA) served as the functional monomer (Merck Chemicals), ethylene glycol dimethacrylate (EGDMA) as the crosslinking agent, and benzoyl peroxide (BPO) as the polymerization initiator (Merck Chemicals). Polyvinyl chloride (PVC) and dioctyl phthalate (DOP) were used for membrane preparation (Sigma Aldrich). Methanol, acetonitrile, glacial acetic acid, dimethyl sulfoxide (DMSO, Merck Chemicals), and deionized water were used as solvents throughout the study and were purchased as HPLC-grade. Potassium chloride (KCl) (Merck Chemicals) was used as the internal electrolyte solution. All chemicals were of analytical grade and used without further purification. Curcumin and amoxicillin (Kalbe Farma) were also used.

Instrumentation

Potentiometric measurements were performed using a high-impedance digital electrometer. The electrode system consisted of a fabricated MIP-based working electrode and an Ag/AgCl reference electrode. Characterization of the synthesized polymers was performed using Fourier-transform infrared spectroscopy (FTIR, Agilent Cary 630) at wave numbers 650–4000 cm^{-1}, scanning electron microscopy (SEM, ZEISS EVO@MA10), and thermogravimetric analysis (TGA, Hitachi STA-7300) with a heating rate of 10 °C/min. A pH meter (Hanna Instruments) was used to adjust the pH. Additional laboratory equipment included an analytical balance, a magnetic stirrer, a heating oven, a vacuum filtration system, and a Soxhlet extraction apparatus.

Procedure

Preparation of non-imprinted polymer (NIP)

All chemical components were mixed sequentially in a beaker consisting of 2.0 mL DMSO, 0.3 mL MMA, 0.5 mL EGDMA, and 0.07 g BPO to form a prepolymer solution. The prepolymer solution was transferred into a synthesis bottle, sealed, and stored in a refrigerator for 1 h. Subsequently, the mixture was heated in an oven at 70 °C for 150 min. Bulk polymerization was considered complete when a solid mass was formed, yielding the NIP [2,18-20].

Preparation of MIP

A prepolymer solution was prepared by sequentially mixing 2.0 mL DMSO, 0.3 mL MMA, 0.5 mL EGDMA, and 0.07 g BPO in a beaker. Separately, 0.22 g of meropenem was dissolved in 2.0 mL DMSO and stirred for 15 min. The meropenem solution was then combined with the prepolymer solution in a synthesis bottle, sealed tightly, and stored in a refrigerator for 1 h to allow pre-complex formation. The mixture was subsequently heated in an oven at 70 °C for 150 min. Polymerization was indicated by the formation

of a solid material, corresponding to the MIP. The resulting MIP was characterized using SEM, FTIR, and TGA [2,21].

Template removal

The MIP was mixed with 10 mL of acetonitrile and allowed to stand for 24 h to facilitate sedimentation. The first washing step was performed using a methanol–glacial acetic acid mixture (85:15, v/v) for one h, and the washing solution was analyzed by UV-vis spectrophotometry. A second wash was performed using a methanol–deionized water mixture (6.0:12.5 mL) for 1 h, followed by UV-vis analysis of the wash solution. The third washing step involved treatment with 3 mL of methanol for 24 h. SEM was employed to observe differences in pore size and to evaluate the effectiveness of template removal, while FTIR was used to confirm its removal [20].

Fabrication of the MIP-based electrode sensor body

The sensor body was prepared from a 12 cm-long 0.5 mm silver wire. An Ag/AgCl wire was placed at the center and fixed in place with resin to cover both wire rods. The wire tip was coated with resin and subsequently polished with sandpaper until the metal surface was exposed.

Immobilization of MIP on the sensor surface

The membrane composition consisted of 32.86% PVC, 57.90% dioctyl phthalate (DOP), and 6.21% meropenem template mixture. The MIP membrane was cast onto a glass surface and allowed to dry at room temperature. The dried MIP membrane layer was then placed on the sensor body surface. The internal filling solution of the electrode consisted of equal volumes of 1×10^{-4} M meropenem solution and 1×10^{-3} M KCl. Prior to use, the electrode was conditioned by soaking overnight in a 1×10^{-4} M meropenem solution. The MIP-coated meropenem sensor was then ready for use [22].

Potentiometric measurements using the MIP sensor

Potentiometric measurements were carried out using a high-impedance digital electrometer connected to the fabricated MIP sensor. Standard meropenem solutions with concentrations ranging from 1×10^{-5} to 1.0×10^{-3} M were prepared. Measurements were performed for each concentration on the first day, and the corresponding potential values were recorded. Measurements were continued for up to 60 d to monitor changes in potential response. The duration over which the sensor exhibited stable potential responses was used to evaluate the operational lifetime of the MIP-based sensor [20].

■ RESULTS AND DISCUSSION

Characterization of NIP, MIP, and MIP Template

FTIR analysis was conducted to validate the establishment of the MMA–EGDMA polymer network and to investigate structural disparities between the template-containing MIP and the NIP. A wide band centered around 3399 cm^{-1} was observed in the FTIR spectrum of the MIP before the template was removed. This band doesn't originate from the hydroxyl (O–H) groups of the monomer because MMA lacks O–H functionalities. Instead, it is more likely related to the N–H or O–H vibrational modes of meropenem molecules trapped in the polymer matrix, or to moisture held via specific interaction sites. The strong carbonyl (C=O) absorption band at 1745 cm^{-1} corresponds to the ester C=O stretching vibrations of MMA and EGDMA. However, its increased intensity and band broadening can be attributed to its overlap with the C=O groups of the β-lactam ring in meropenem [23].

The presence of the meropenem template was further confirmed by distinctive bands in the 1550–1650 cm^{-1} range, linked to amide vibrations and the heterocyclic β-lactam structure—bands that were not present in the NIP spectrum. These bands disappeared after template extraction, and the carbonyl absorption intensity returned to a pattern similar to that of the NIP. This showed that meropenem had been successfully removed from the polymer network (Fig. 1). The NIP spectrum, on the other hand, only showed the MMA–EGDMA polymer matrix. It had a sharp, symmetrical peak at 1745 cm^{-1}, indicating the presence of ester C=O groups [24].

SEM was used to examine the surface morphology of the NIP, the template-containing MIP, and the MIP after template extraction. The three materials showed clear

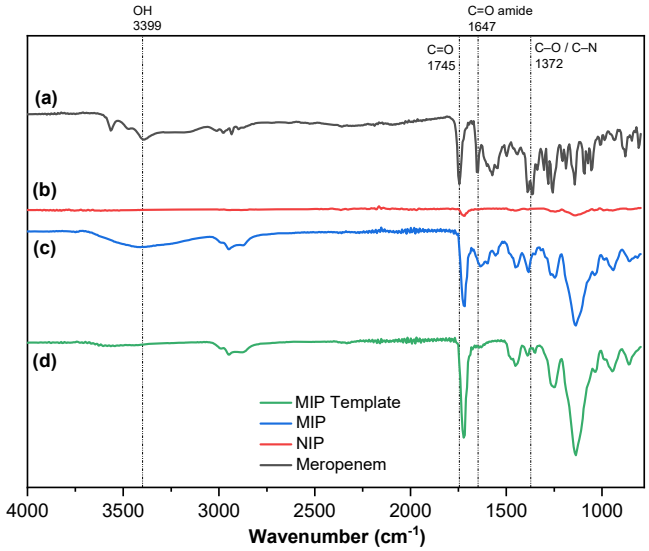

Fig 1. FTIR spectra of (a) meropenem, (b) NIP, (c) MIP containing meropenem before template extraction (MIP–template), and (d) MIP after template extraction

morphological differences, indicating that polymer formation and template extraction influenced the bulk surface structure (Fig. 2).

The NIP exhibited a relatively dense and compact surface with limited visible porosity, consistent with polymer formation in the absence of a template molecule. In contrast, the template-containing MIP exhibited a more irregular, heterogeneous morphology, suggesting that meropenem affected the organization of the polymer matrix during polymerization [2,25].

The MIP with the template (template-in), on the other hand, had a much more uneven surface, with large aggregates and irregular cavities that appeared to be partially blocked. This morphology suggests that the template influenced the bulk organization of the polymer during polymerization, resulting in a less open surface after template extraction. Before template extraction, numerous reports have shown that MIPs exhibit bulk-like morphologies that are similar to one another. This is because template molecules in the polymer matrix block the formation of pores [26-27].

After template extraction, the MIP exhibited a more open, porous surface. However, because the SEM micrographs were obtained at 1,000× magnification, the

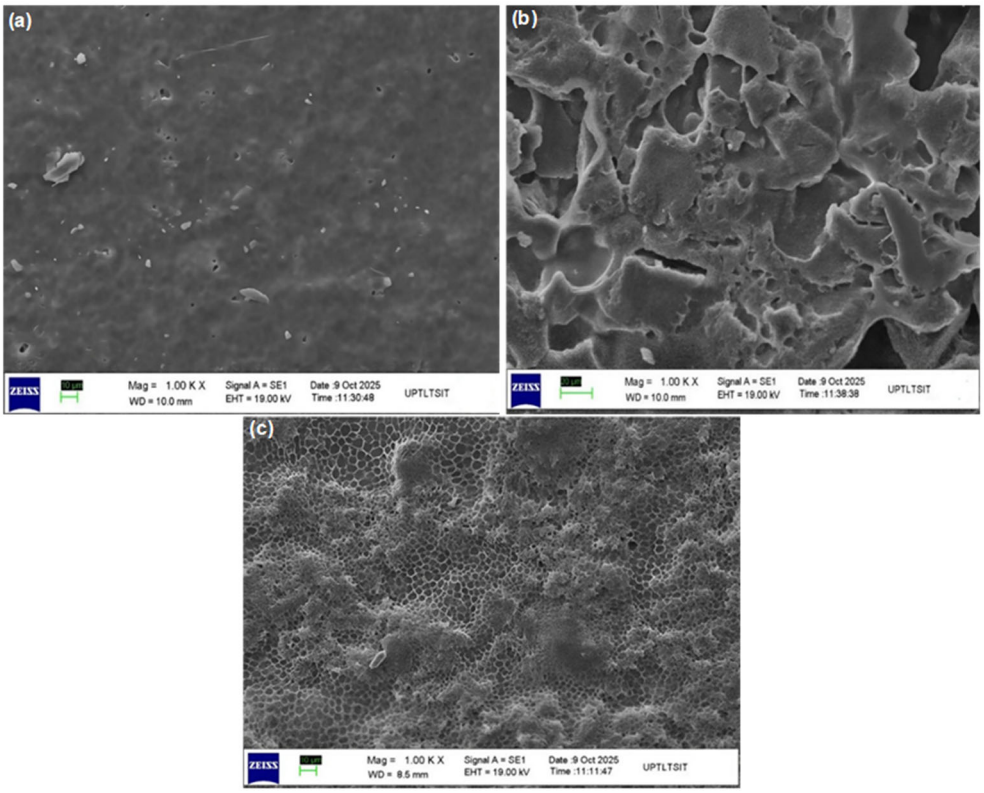

Fig 2. SEM micrographs of (a) NIP, (b) MIP containing meropenem before template extraction (MIP–template), and (c) MIP after template extraction

observed pores should be interpreted as micrometer-scale bulk morphological features rather than direct visualization of molecular-scale imprint cavities. Therefore, the SEM analysis in Fig. 2 provides evidence of morphological changes associated with imprinting and extraction, but not direct proof of template-sized binding sites [20,28].

These pores are a unique feature of well-formed MIPs, and having more of them makes it easier for the MIPs to bind to the target analyte. In general, the SEM results show that the NIP, the template-containing MIP, and the extracted MIP have very different shapes. Overall, the SEM results support the occurrence of morphological differences between NIP, template-containing MIP, and extracted MIP. These observations are consistent with structural changes during imprinting and extraction, whereas selective recognition is better supported by the combined FTIR and potentiometric performance results [29].

The TGA results in Fig. 3 strongly support the FTIR and SEM results, as the differences in how the NIP, template-containing MIP, and extracted MIP decompose upon heating indicate that the structure has changed in a manner consistent with the molecular imprinting process. The MIP with the template broke down thermally earlier than the NIP did. This was because the meropenem in the matrix reduced the polymer network's density. This finding aligns with the FTIR results, which still showed the characteristic amide and heterocyclic bands of meropenem, and with the SEM images, which revealed a dense, non-porous surface morphology.

After template extraction, the TGA profile of the MIP shifted toward that of the NIP, although the extracted MIP still exhibited slightly lower thermal stability [20]. This behavior is consistent with the disappearance of meropenem-related bands in the FTIR spectra and the SEM observations, which reveal a porous surface with well-formed imprint cavities. The formation of these cavities inherently increases the polymer's

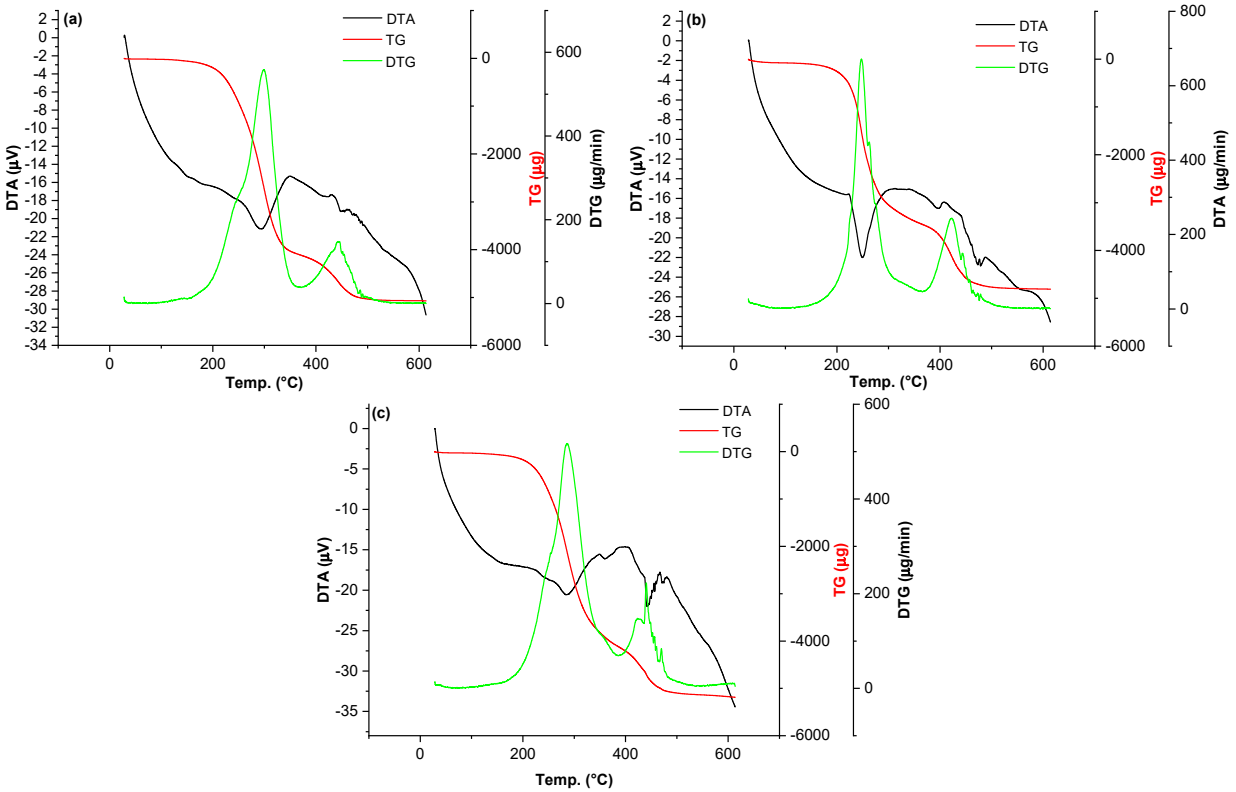

Fig 3. TGA and derivative thermogravimetric (DTG) curves of (a) NIP, (b) MIP containing meropenem before template extraction (MIP–template), and (c) MIP after template extraction

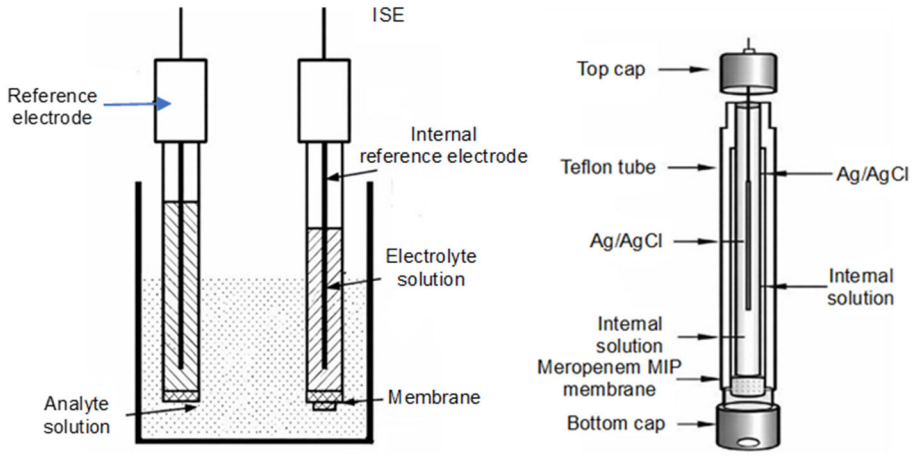

Fig 4. Ion-selective electrode schematic diagram

susceptibility to thermal degradation, as it increases porosity and reduces network density.

Potentiometric Performance Evaluation

A schematic diagram of the ion-selective electrode (ISE) system used in this study is shown in Fig. 4. The configuration includes the reference electrode, the internal Ag/AgCl system, the electrolyte solution, and the MIP-based selective membrane in contact with the analyte solution. The potentiometric response arises from the potential difference across the membrane due to selective interaction with meropenem, enabling conversion of chemical activity into an electrical signal measured by a digital electrometer.

The calibration plot (Fig. 5) shows a linear relationship between the measured potential (EMF) and the logarithm of meropenem concentration over the investigated range. The sensor exhibited a near-Nernstian slope of 54.87 mV per decade with a correlation coefficient (R^2) of 0.995, indicating good linearity of response. A linear response was observed over the concentration range of 1.0×10^{-5} to 1.0×10^{-3} M, defined here as the working range of the sensor under the applied experimental conditions.

The limit of detection (LOD) and limit of quantification (LOQ) were calculated based on the standard deviation of the analytical response and the slope of the calibration curve. The calculations were performed using the relationships LOD = 3.3σ/S and LOQ = 10σ/S, where σ represents the standard deviation of the response, and S is the slope of the calibration plot.

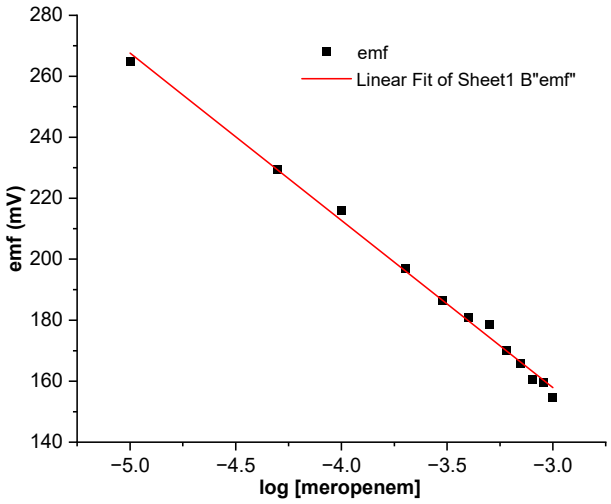

Fig 5. Potentiometric calibration curve of the MIP-based meropenem sensor showing the relationship between electrode potential (mV) and the logarithm of meropenem concentration

Potentiometric measurements were conducted in triplicate (n = 3) at each concentration level. The standard deviation (σ) used in the calculation was obtained from replicate measurements at low concentration levels, where signal variability is most representative of the detection limit. Based on the recalculated raw experimental data, the standard deviation at low concentrations was approximately 0.85 mV. Using this approach and a calibration slope of 54.87 mV per decade, the recalculated LOD and LOQ values were 1.12×10^{-5} and 1.43×10^{-5} M, respectively.

The LOQ is higher than the LOD, as expected, because the LOQ represents the minimum concentration that can be quantified with acceptable precision and accuracy. In contrast, the LOD represents only the minimum detectable signal.

The proximity of the lowest calibration concentration to the LOQ indicates that measurements in this region approach the lower limit of reliable quantification. Nevertheless, the calibration plot remained linear across the investigated range. Residual analysis showed a random distribution around zero, supporting the suitability of the linear regression model. This approach is consistent with commonly accepted analytical method validation practices [20].

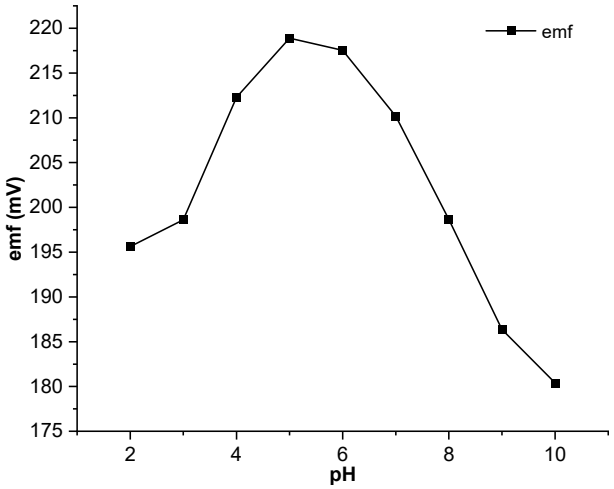

Fig 6. Effect of solution pH on the potentiometric response of the MIP-based meropenem sensor

Effect of pH

The potentiometric response of the MIP–meropenem ion-selective electrode showed a distinct pH dependence. The observed increase in potential from pH 2.0 to 5.0 can be attributed to alterations in meropenem speciation, wherein excessive protonation at low pH diminishes the proportion of negatively charged species and weakens electrostatic interactions with the MIP recognition sites, resulting in reduced EMF responses. The best and most stable potentiometric signals were observed at pH 5.0–6.0, where meropenem predominantly exists in an anionic form under mildly acidic to near-neutral conditions (Fig. 6). This enables optimal hydrogen bonding and electrostatic interactions with the imprinted cavities. This stability indicates a good ionic balance at the membrane–solution interface. When the pH is above 6.0, the response goes down because hydroxide ions compete with each other, and the β-lactam structure becomes less stable in alkaline conditions. This alters the charge distribution, making it harder for the MIP sites to bind the β-lactam. In general, these results show that pH is an important factor in improving the performance of the MIP-based sensor in potentiometric measurements [30-31].

The observed slope is close to the theoretical Nernstian value of approximately 59 mV per decade for a monovalent ion at 25 °C. However, meropenem is an amphoteric molecule containing multiple ionizable functional groups, and its charge state depends on the solution pH. At pH 5–6, meropenem is expected to exist predominantly in a partially ionized form, resulting from the balance between its acidic and basic functional groups. This pH-dependent ionization behavior may lead to slight deviations from an ideal Nernstian response. Therefore, the obtained slope is interpreted as a near-Nernstian response under the applied experimental conditions, reflecting the combined effects of ionization equilibria and membrane interactions. The high linearity ($R^2 = 0.995$) indicates that the sensor provides a consistent, reliable response over the studied concentration range [20].

Response Time

The analyte concentration in the test solution had a significant effect on the rate of response of the MIP–meropenem potentiometric sensor. Dynamic response data across three concentration levels showed that elevated meropenem concentrations led to shorter response times and higher steady-state potentials. This phenomenon can be ascribed to an augmented ionic activity gradient and a more rapid attainment of ionic equilibrium at the membrane–solution interface. When the concentrations were lower, the ion flow toward the membrane surface was limited, making diffusion and binding at the MIP recognition sites the rate-limiting steps, resulting in slower sensor response. In contrast, at medium to high concentrations, the higher number of

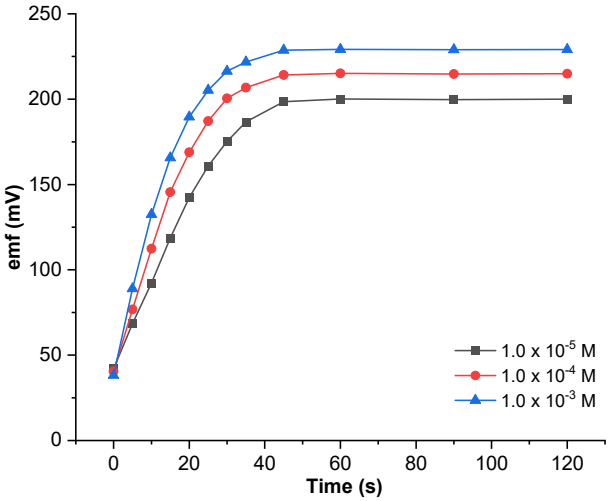

Fig 7. Dynamic potentiometric response of the MIP-based meropenem sensor

ionic species accelerated ion exchange and selective binding within the imprinted cavities. This allows the sensor to reach approximately 95% of the equilibrium potential in about 45 s (Fig. 7). The stable, steady-state signals, which lasted up to 120 s, further demonstrate that the PVC–MIP membrane exhibits good ion-transport properties and that analyte–MIP interactions are rapid and reversible. This indicates that the sensor is suitable for rapid potentiometric analysis [20,30].

Repeatability, Stability, and Sensor Lifetime

The reliability of polymeric membrane-based potentiometric sensors in routine analysis can be assessed by their repeatability, stability, and durability. This study evaluated the repeatability of the MIP–meropenem sensor by performing multiple measurements at a constant concentration, yielding low %RSD values and indicating high precision. This behavior indicates that the interaction between meropenem and the recognition sites in the MIP cavities is stable and reversible. This means that the potentiometric responses are the same every time they are measured under the same conditions. The absence of significant signal drift after equilibrium was reached further confirmed short-term stability. This indicates that the PVC–MIP membrane can maintain ionic equilibrium and facilitate efficient ion transport at the membrane–solution interface.

The sensor was monitored for 60 d; however, stable near-Nernstian performance was maintained for up to 50 d, which was therefore defined as the effective operational lifetime (Table 1). After this time, the sensitivity slowly decreased, and the potential drift increased. This was likely due to membrane aging, leading to plasticizer leaching, less flexible membranes, and partial deformation or blockage of the MIP recognition cavities. In general, the integrated repeatability, stability, and lifetime results show that the MIP-meropenem sensor works reliably and consistently for quantitative analysis over a medium-term operational period. This is similar to or better than what has been reported for other MIP-based potentiometric sensors in the literature [20,30,32].

Table 1. Operational lifetime of the MIP-based meropenem potentiometric sensor

Day	Slope (mV/decade)	EMF at 1.0×10^{-4} M (mV)
0	54.9	215.0
5	54.8	214.9
10	54.9	214.8
15	54.7	214.7
20	54.8	214.6
25	54.6	214.5
30	54.7	214.3
35	54.6	214.1
40	54.5	213.9
45	54.4	213.7
50	54.3	213.4
55	53.7	212.0
60	52.9	210.8

Selectivity Evaluation Using the MPM

The selectivity of the proposed sensor was evaluated using the MPM, a widely used method for assessing the influence of interfering species in potentiometric systems. This method compares the change in electrode potential (ΔE) produced by the primary analyte with that produced by an interfering species under equivalent conditions. In this approach, the potentiometric selectivity coefficient is expressed as a dimensionless parameter, $K_{i,j}^{MPM}$, which reflects the relative response of the sensor toward the interfering species compared to the primary ion. The selectivity coefficient is calculated using Eq. (1);

$$K_{i,j}^{MPM} = \frac{\Delta a_i}{a_j} \quad (1)$$

where Δa_i is the increment in the concentration (or activity) of the primary ion required to produce a defined ΔE change, and a_j is the concentration (or activity) of the interfering species that produces the same potential change. The MPM approach does not require the assumption of ideal Nernstian behavior. It is therefore more suitable for evaluating selectivity in non-ideal systems, including sensors based on MIPs and complex pharmaceutical analytes [32-34].

Amoxicillin and curcumin were selected as interfering species to evaluate the selectivity of the proposed sensor under different structural conditions. Amoxicillin was chosen as a structurally relevant interferent because it belongs to the β-lactam class of antibiotics and shares key structural features with meropenem. In contrast, curcumin was selected as a structurally unrelated compound to represent a chemically distinct species.

The selectivity coefficients obtained using the MPM are summarized in Table 2. The results indicate that the sensor response is influenced by the structural similarity of the interfering species to meropenem. In particular, the selectivity coefficient obtained for amoxicillin ($K_{i,j}^{MPM}$ = 111) indicates a comparable response, suggesting limited discrimination against structurally related β-lactam compounds. This behavior is reasonable, as structural similarities between amoxicillin and meropenem may lead to similar interactions with the imprinted binding sites.

In contrast, the lower selectivity coefficient observed for curcumin ($K_{i,j}^{MPM} < 1$) indicates better discrimination toward a structurally unrelated compound. These results suggest that the molecular imprinting process contributes to analyte recognition; however, the degree of selectivity is strongly influenced by the structural similarity between the target analyte and potential interfering species. Overall, the selectivity of the proposed sensor is more appropriately described as moderate. The sensor exhibits improved discrimination toward structurally dissimilar compounds, while interference from structurally related β-lactam antibiotics may still occur [32,35].

Table 2. Potentiometric selectivity coefficients of the MIP-based meropenem sensor determined by MPM

Species	Concentration (M)	Interferent activity, a_j (M)	K_{ij}^{MPM}
Meropenem (i)	2.0×10^{-5}	–	–
Amoxicillin (j)	2.0×10^{-5}	1.8×10^{-5}	1.11
Curcumin (j)	2.0×10^{-5}	6.5×10^{-5}	0.31

Comparison with Previously Reported Methods

To better position the proposed sensor within the current state of the art, a comparison with previously reported methods for meropenem determination is summarized in Table 3. As shown in Table 3, chromatographic techniques such as HPLC provide high sensitivity and accuracy but require complex instrumentation and sample preparation. Voltammetric sensors offer improved detection limits, often enhanced by nanomaterial modifications; however, these approaches typically involve more complicated electrode fabrication procedures.

In contrast, the MIP-based potentiometric sensor developed in this study offers a simpler and more cost-effective alternative. Although its detection limit is higher than that of advanced electrochemical sensors, it provides acceptable analytical performance with advantages in ease of operation, rapid response, and potential applicability for routine analysis. Therefore, the proposed method does not aim to outperform existing techniques in terms of sensitivity, but rather to provide a complementary analytical approach that emphasizes simplicity and practicality.

As shown in Table 3, the proposed sensor does not provide the lowest detection limit compared to advanced HPLC or voltammetric methods. Voltammetric sensors based on nanomaterial-modified electrodes can achieve lower detection limits, typically in the range of 10^{-6} to 10^{-9} M. In contrast, the proposed potentiometric sensor exhibits a higher LOD (1.12×10^{-5} M), reflecting differences in its detection mechanism. However, it offers a simpler and more cost-effective approach with acceptable analytical performance.

Table 3. Comparison of analytical methods for meropenem determination

Method	Electrode/Technique	Linear range	LOD	Sample matrix	Key features	Ref
HPLC	RP-HPLC	µg/mL range	~µg/mL	Plasma, pharmaceutical	High accuracy, robust	[4]
Voltammetry (DPV/CV)	CNT-modified electrode	3.0×10^{-7}–7.0×10^{-5} M	1.5×10^{-6} M	Plasma	High sensitivity, but complex modification	[12]
Voltammetry (nano-based sensor)	Fe–Ni/CNT modified GCE	0.01–12 µM	1.3 nM	Human serum	Very low LOD, multi-layer fabrication	[11]
MOF-based electrochemical sensor	Cu/Ni-MOF modified electrode	~10^{-7} M range	~10^{-6} M	Plasma	Enhanced sensitivity via nanomaterials	[13]
Voltammetry (graphene composite)	PAN/Graphene/GCE	2.5×10^{-7}–3.5×10^{-4} M	3.6×10^{-9} and 1.75×10^{-9} M for DPM and MPM, respectively	Urine, serum	Wide linear range, good sensitivity	[36]
Electrochemical sensor (DPV)	GC/Gr/CNT-HQ/Fe-Ni) electrode	LN (0.007–12 µM) and ME (0.01–12 µM)	0.97 nM for LN and 1.3 nM for ME	Human blood serum	High sensitivity, enhanced oxidation current, rapid response, suitable for therapeutic drug monitoring	[11]
This work	MIP-based potentiometric ISE	1.0×10^{-5}–1.0×10^{-3} M	1.12×10^{-5} M	Standard solution	Simple, low-cost, rapid response, selective recognition via MIP	This study

■ CONCLUSION

A MIP-based potentiometric ISE for the detection of meropenem. The sensor exhibited a near-Nernstian response with a slope of 54.87 mV per decade and good linearity over the concentration range of 1.0×10^{-5} to 1.0×10^{-3} M ($R^2 = 0.995$). The calculated LOD and LOQ were 1.12×10^{-5} and 1.43×10^{-5} M, respectively, indicating acceptable analytical sensitivity under the studied conditions. The sensor demonstrated a rapid response time of approximately 45 s, optimal performance within the pH range of 5.0–6.0, and operational stability for up to 50 d. Selectivity evaluation using the matched potential method indicated moderate selectivity, with noticeable interference from structurally related β-lactam antibiotics such as amoxicillin, while better discrimination was observed for structurally unrelated compounds. SEM morphological characterization revealed differences in bulk surface structure between NIP and MIP materials following template extraction; however, the observed features correspond to micrometer-scale morphology and do not directly represent molecular imprinting cavities. The presence of selective recognition sites is therefore supported by the combined evidence from template removal, FTIR characterization, and potentiometric performance. Overall, the developed sensor provides a simple, low-cost, and rapid analytical platform for meropenem detection, with performance comparable to that of more complex electrochemical methods. Nevertheless, further validation using real samples, including pharmaceutical wastewater and biological matrices such as plasma, is required to assess matrix effects and recovery performance, and these studies are currently underway as part of ongoing research.

■ ACKNOWLEDGMENTS

The authors express their gratitude to the Directorate of Research and Community Service, Directorate General of Research and Development, Ministry of Higher Education, Science, and Technology of the Republic of Indonesia (*DRTPM Kemdiktisaintek*) for financial assistance through the Higher Education Research Program, which supports the Beginner Lecturer Research (PDP) scheme conducted in 2025. This research was financed through the principal contract No. 122/C3/DT.05.00/PL/2025, dated May 28, 2025, the first derivative contract No.

49/SPK/LL1/AL.04.03/PL/2025, dated June 11, 2025, and the second derivative contract No. 014/AK/LM/INKES-MLP/VI/2025, dated June 12, 2025.

■ CONFLICT OF INTEREST

The authors have no conflict of interest.

■ AUTHOR CONTRIBUTIONS

Herlina, Ahmad Hafizullah Ritonga, Andy Febriady, Barita Aritonang, Reynaldo Sinaga, and Amelia Sundari contributed to materials preparation, analytical support, and conducted the experiment. Herlina, Asvia Rahayu, and Muhammad Razali assisted with the calculations, analysis, and validation. Herlina wrote the manuscript. Herlina, Ahmad Hafizullah Ritonga, and Barita Aritonang critically revised the manuscript for important intellectual content. All authors have read and approved the final version of the manuscript.

■ REFERENCES

[1] Barathe, P., Kaur, K., Reddy, S., Shriram, V., and Kumar, V., 2024, Antibiotic pollution and associated antimicrobial resistance in the environment, *J. Hazard. Mater. Lett.*, 5, 100105.

[2] Sirumapea, L., Zulfikar, M.A., Amran, M.B., and Alni, A., 2021, Selective solid-phase extraction of meropenem from human blood plasma using a molecularly imprinted polymer, *Indones. J. Chem.*, 21 (5), 1167–1179.

[3] Steffens, N.A., Zimmermann, E.S., Nichelle, S.M., and Brucker, N., 2021, Meropenem use and therapeutic drug monitoring in clinical practice: A literature review, *J. Clin. Pharm. Ther.*, 46 (3), 610–621.

[4] Ren, X., Ye, J., Chen, X., Wang, F., Liu, G., and Wang, J., 2021, Development of a novel HPLC method for the analysis of impurities in meropenem and identification of unknown impurities by 2D LC-IT-TOF MS, *Chromatographia*, 84 (10), 937–947.

[5] Bashimam, M., and El-Zein, H., 2024, Development and validation of a green RP-HPLC method for detection and quantitation of meropenem trihydrate in the bulk: A comparison with HPTLC method, *Curr. Chem. Lett.*, 13 (2), 351–358.

[6] Jin, Y., Ma, H., Fu, L., Qi, X., Zhang, M., Di, X., Zheng, L., He, C., and Wang, Z., 2024, Quantification of meropenem in serum and cerebrospinal fluid in children with bacterial meningitis with augmented renal clearance by UPLC–MS/MS, *Heliyon*, 10 (4), e26132.

[7] Wilk, J., Sowik, P., Felis, E., Harnisz, M., Korzeniewska, E., and Bajkacz, S., 2025, Development SPE-LC-MS/MS method for determination of WHO AWaRe Reserve antibiotics in hospital wastewater, *Sci. Rep.*, 15 (1), 22163.

[8] Narala, S.R., and Saraswathi, K., 2023, Extractive spectrophotometric determination of meropenem in pharmaceutical formulations, *Res. J. Pharm. Technol.*, 16 (9), 4148–4150.

[9] Shuker Mahmood, H., and Mahmood, A.H., 2023, A new spectrophotometric approach for determination of meropenem in pharmaceutical formulation, *Rafidain J. Sci.*, 32 (3), 9–20.

[10] Harsini, M., Farida, A.N., Fitriany, E., Paramita, D.R.A., Baktir, A., Kurniawan, F., Sakti, S.C.W., Kurniawan, Y.D., Widyaningrum, B.A., 2024, Simultaneous analysis of dopamine and ascorbic acid using polymelamine/gold nanoparticle-modified carbon paste electrode, *Indones. J. Chem.*, 24 (1), 38–53.

[11] Atta, N.F., Galal, A., and El-Gohary, A.R.M., 2021, Novel designed electrochemical sensor for simultaneous determination of linezolid and meropenem pneumonia drugs, *J. Electroanal. Chem.*, 902, 115814.

[12] Atta, M.Y., Hegazy, M.A., Mahmoud, A.M., and Ghoniem, N.S., 2022, Electrochemical sensor for meropenem therapeutic monitoring in human plasma based on carbon nanotubes modified basal pyrolytic graphite electrode, *J. Electrochem. Soc.*, 169 (9), 097504.

[13] Ali, S.N., Mahmoud, A.M., Saad, S.S., Fayed, A.S., and Marzouk, H.M., 2025, A novel bimetallic metal–organic framework-based electrochemical nanosensor for therapeutic monitoring of meropenem in human plasma, *Microchem. J.*, 215, 114184.

[14] Khasanah, M., Widati, A.A., Handajani, U.S., Harsini, M., Ilmiah, B., and Oktavia, I.D., 2020, Imprinted zeolite modified carbon paste electrode as a selective sensor for blood glucose analysis by potentiometry, *Indones. J. Chem.*, 20 (6), 1301–1310.

[15] Djunaidi, M.C., Afriani, M.D.R., Gunawan, G., and Khasanah, M., 2021, Synthesis of graphite paste/molecularly imprinted polymer (MIP) electrodes based on polyeugenol as a glucose sensor with potentiometric method, *Indones. J. Chem.*, 21 (4), 816–824.

[16] Wang, J., Liang, R., and Qin, W., 2024, Improvement of the selectivity of a molecularly imprinted polymer-based potentiometric sensor by using a specific functional monomer, *Anal. Chim. Acta*, 1298, 342412.

[17] Ammen, E.W., and Al-Bayati, Y.K., 2024, Determination of chlorpromazine using molecular imprinting polymers in different sample matrices, *Indones. J. Chem.*, 24 (6), 1870–1882.

[18] Ma, X., Wang, Y., Wang, W., Heinlein, J., Pfefferle, L.D., and Tian, X., 2023, Strategic preparation of porous magnetic molecularly imprinted polymers via a simple and green method for high-performance adsorption and removal of meropenem, *Talanta*, 258, 124419.

[19] Özbek, O., Berkel, C., and Isildak, Ö., 2022, Applications of potentiometric sensors for the determination of drug molecules in biological samples, *Crit. Rev. Anal. Chem.*, 52 (4), 768–779.

[20] Majdi, M., Mizani, F., and Mohammad-Khah, A., 2022, Quantitative monitoring of cefotaxim ions by a new potentiometric sensor based on molecularly imprinted polymer, *Anal. Bioanal. Electrochem.*, 14 (1), 100–115.

[21] Bow, Y., Syakdani, A., Purnamasari, I., and Rusdianasari, R., 2023, Electrochemical sensor based on molecularly imprinted polymer (MIP) for simazine pesticide detection, *Int. J. Adv. Sci., Eng. Inf. Technol.*, 13 (1), 110–116.

[22] Mahmoud, A.M., Saleh, H., Fawzy, M.G., Reda, A., and Bahgat, E.A., 2024, Design of potentiometric sensor based on molecularly-imprinted polymer for direct detection of levofloxacin in plasma for point-of-care applications, *Zagazig J. Pharm. Sci.*, 33 (1), 38–48.

[23] Amlashi, H.S., Daryasari, A.P., and Soleimani, M., 2019, Molecularly imprinted polymer solid phase extraction followed by high-performance liquid chromatography as an efficient and sensitive technique for determination of meropenem in human plasma and urine, *S. Afr. J. Chem.*, 72, 32–39.

[24] Serag, A., Abdelazim, A.H., Ramzy, S., Alnemari, R.M., Alzhrani, R.M., Abduljabbar, M.H., Althobaiti, Y.S., Alosaimi, M.E., Alaqel, S.I., and Almalki, A.H., 2026, A fluorescent sensor based on nitrogen-doped graphene quantum dots and molecularly imprinted polymers for selective and sensitive detection of meropenem in environmental and clinical matrices, *Talanta*, 296, 128442.

[25] Yence, M., Cetinkaya, A., Çorman, M.E., Uzun, L., Caglayan, M.G., and Ozkan, S.A., 2023, Fabrication of molecularly imprinted electrochemical sensors for sensitive codeine detection, *Microchem. J.*, 193, 109060.

[26] Wang, L., and Zhang, W., 2023, Molecularly imprinted polymer (MIP) based electrochemical sensors and their recent advances in health applications, *Sens. Actuators Rep.*, 5, 100153.

[27] Ahmed, E.R., Abou-Elella, F.M., Abdelmonem, A.M., and Ali, M.A., 2025, Resveratrol-loaded magnetic molecularly imprinted polymers: A green dual-functional platform for synergistic antibacterial and targeted anticancer therapy, *Chem. Biol. Technol. Agric.*, 12 (1), 171.

[28] Banerjee, R., and Bhattacharya, T., 2022, Degradation of synthetic polymers: Microbial approach, *Indian J. Microbiol. Res.*, 9 (1), 9–13.

[29] Khudhair, M.B., and Al-Phalahy, B.A., 2020, New potentiometric sensor for levofloxacin determination in pharmaceutical preparations, urine and blood serum, *Biochem. Cell. Arch.*, 20, 6101–6107.

[30] Parshina, A., Yelnikova, A., Safronova, E., Kolganova, T., Bobreshova, O., and Yaroslavtsev, A., 2023, Potentiometric sensor arrays based on hybrid PFSA/CNTs membranes for the analysis of UV-degraded drugs, *Polymers*, 15 (12), 2682.

[31] Moaaz, E.M., Fayed, A.S., Abdel-Moety, E.M., and Rezk, M.R., 2025, Innovative sensors with selectivity enhancement by molecularly imprinted polymers for the concurrent quantification of donepezil and memantine, *RSC Adv.*, 15 (23), 18475–18489.

[32] Ibrahim, E.A., Saad, S.S., Hegazy, M.A., Abdel Fattah, L.E., and Marzouk, H.M., 2025, A novel molecular imprinted polymer-based potentiometric sensor for determination of the neuromodulating drug safinamide in dosage form and biological fluids, *Microchem. J.*, 214, 114059.

[33] Wang, C., Qi, L., and Liang, R., 2021, A molecularly imprinted polymer-based potentiometric sensor based on covalent recognition for the determination of dopamine, *Anal. Methods*, 13 (5), 620–625.

[34] Djunaidi, M.C., Gunawan, G., Cahyaningrum, L., Lusiana, R.A., and Khasanah, M., 2022, Selective identification for glucose in the presence of fructose using imprinted polyeugenol modified graphite paste electrode, *Indones. J. Chem.*, 22 (4), 913–921.

[35] Sirumapea, L., Ali Zulfikar, M., Bachri Amran, M., and Alni, A., 2019, Synthesis and characterization of meropenem imprinted polymer, *J. Phys.: Conf. Ser.*, 1282 (1), 012063.

[36] Sivaprasad, M., Swarupa, C., Dhananjayulu, M., Jayapal, M.R., and Sreedhar, N.Y., 2014, Graphene and polyaniline composite modified glassy carbon electrode for electrochemical determination of doripenem and meropenem metabolites, *J. Anal. Bioanal. Tech.*, 5 (3), 1000192.